CHEMISTRY
A European Journal

A Journal of
ChemPubSoc Europe

Accepted Article

Title: Selective Dual-Channel Imaging on Cyanostyryl-Modified Azulene Systems with Unimolecularly Tunable Visible-Nearinfrared Luminescence

Authors: Yunyun Zhou and Liangliang Zhu

To be cited as: *Chem. Eur. J.* 10.1002/chem.201700947

Link to VoR: http://dx.doi.org/10.1002/chem.201700947

Supported by
ACES

WILEY-VCH

10.1002/chem.201700947

COMMUNICATION

WILEY-VCH

Selective Dual-Channel Imaging on Cyanostyryl-Modified Azulene Systems with Unimolecularly Tunable Visible-Nearinfrared Luminescence

Yunyun Zhou,[a] Yaping Zhuang,[a] Xin Li,[b] Hans Ågren,[b] Lin Yu,[a] Jiandong Ding,[a] and Liangliang Zhu*[a]

Abstract: While organic light-emitting molecules have received a growing attention and applicability in modern bioimaging science, the design and control of complex photoluminescent properties in unimolecularly selective imaging remains a challenging topic. Since tunable multipathway imaging can be advantagedly connected with treatment processes in therapy, we here report the integration of an azulene and a cyanostyryl moiety into one skeleton for the generation of in situ stimuli-responsive luminescent materials, with the aim to achieve tunable and effective emissions in distinct channels via smart molecular design on a single-molecular platform. This strategy takes advantage of 1) the *Z/E* isomerization of the cyanostyryl unit that can vary the push-pull effect of the substitution on azulene, accompanied by altering absorption and emission of individual excited states, and 2) an optimized excited-state regulation for opening a nearinfrared emissive channel and making up for a controllable dual-pathway luminescent system together with the utilization of visible emission. As exemplified by a demonstration of manipulating the luminescence at the cell level, the materials exhibit a superior application potential for unimolecularly selective imaging, labeling and probing events.

Microscale and nanoscale photoluminescent techniques have enabled a grand scientific advancement in bioimaging and biosensing.[1] Among such techniques, those involving materials with nearinfrared (NIR) luminescence have attracted considerable attention as alternative to visible (Vis) light that is readily hampered by the biological self-luminescent signals and the limited ability to penetrate in vivo.[2] Although the past years have witnessed extensive progress in the NIR luminescent systems for different biomedical applications,[3] the material design and choice still face with challenges at the molecular level. For examples, the generation of NIR emission has largely relied on big and planar π conjugated structures.[4] To seek simple but rational structural strategy for generating and tuning of NIR emissions on a unimolecular scaffold, so as to build a straightforwardly controllable dual-pathway luminescent system together with the utilization of Vis emission, remains a difficult but desirable proposition.

Azulene, a typical dipolar molecule consisting of an electron-deficient 7-membered ring and an electron-rich 5-membered ring is well known for its particular organization of excited states and optical tranisitions.[5] Azulene is prone to emit from the S_2 or higher states thus disobeying Kasha's rule.[6] Such a high-energy radiative decay largely constrains the corresponding emission wavelength within a UV-Vis spectral region. Although the regiochemistry with different substitutions on azulene, interestingly, can help to regulate the S_1-S_2 energy gap so as to vary the absorption behaviour,[7] the characteristics of the NIR emissive pathways for azulene and its derivatives have been only rarely reported..

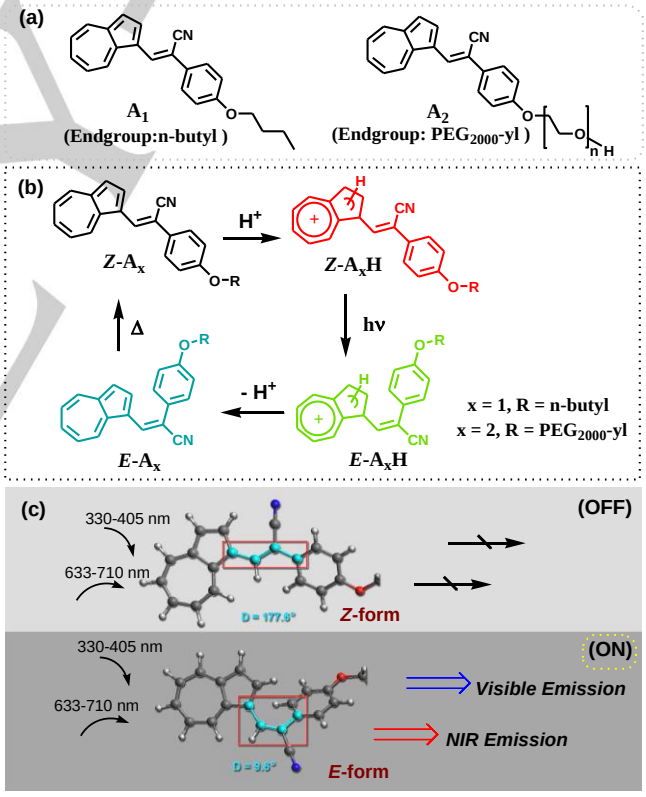

Figure 1. (a) Chemical structures of the cyanostyryl-modified azulenyl compounds $\mathbf{A_1}$ and $\mathbf{A_2}$ and the (b) protonation-assistant photoisomerization process. (c) Optimized conformational (up) *Z*- and (down) *E*-forms of the cyanostyryl-modified azulenyl moiety at the B3LYP/6-31G* level of theory and the illustration of the tunable dual-pathway emission behaviors: the Vis and NIR emissions are both quenched in *Z*-form whereas both strengthened in *E*-form.

We herein put forward an excited-state regulation approach, as well as the role of structural rigidity for the azulene system, to address the possibility of a dual-pathway (Vis and NIR) emission.

[a] Dr. Y. Zhou, Ms. Y. Zhuang, Dr. L. Yu, Prof. Dr. J. Ding, Prof. Dr. L. Zhu
State Key Laboratory of Molecular Engineering of Polymers
Department of Macromolecular Science
Fudan University, Shanghai 200433 china
E-mail: zhuliangliang@fudan.edu.cn
[b] Dr. X. Li, Prof. Dr. H. Ågren
Division of Theoretical Chemistry and Biology
School of Biotechnology
KTH Royal Institute of Technology
SE-10691 Stockholm, Sweden

Supporting information for this article is given via a link at the end of the document.

10.1002/chem.201700947

Cyanostilbene, a polar light-active moiety, provides a tunable push-pull effect through molecular derivation and *Z*/*E*-isomerization, accompanied by the adjustment of its emission wavelength and intensity.[8] As the first publication of this series of work, we demonstrate a unimolecular strategy by combining azulene and cyanostyryl units into one skeleton for a realization of the above-mentioned hypothesis from perspective of precisely regulating π-electron. We expect that a dual-pathway luminescent system can be built in this way, on accounts of the excited-state regulation and conformational control via stimuli-responsive push-pull effect to enable versatile electron-transition processes.

The demonstrated π-functional skeleton was synthesized by knoevenagel condensation within only three steps, leaving a phenolic hydroxyl endgroup for additional derivatizations. In this work, a n-butyl group is introduced for fundamental photochemical and photophysical studies in organic solution (compound **A_1**), whereas a PEG_{2000}-yl chain, a modified poly(ethylene glycol) (PEG), is linked to facilitate the water solubility and biocompatibility for cell imaging (compound **A_2**). Figure 1 outlines the chemical structures as well as the protonation-assistant photoisomerization process of the two compounds. Their preparation route and details are referenced in Experimental Section and Supporting Information (SI).

At the initial state, the cyanostyryl-modified azulene structure adopts a *Z*-form evidenced by well-assigned ^{1}H NMR signals (Figure 2a and S2). Unfortunately, direct photoisomerization was not observed upon irradiation on *Z*-**A_1** either by UV or visible light (see the unchanged NMR or optical spectra in Figure S2 and S3), probably because the azulene moiety quenched the intermediate triplet formation making the photoisomerization insensitive.[9] However, azulene can exhibit stimuli-responsive behavior in acidic environments[5-7,10]. Hence we turn to investigate the synergy effect of pH and light on our compounds.

Upon addition of trifluoroacetic acid (TFA) into *Z*-**A_1** solution, the resonances of proton 2, 3, 4, 5, 8 on the cyanostyryl and 7-membered rings of azulene underwent a downfield shift in the ^{1}H NMR spectra, whereas that of proton 1 on 5-membered ring experienced an upfield shift and proton 7 turned broad (see Figure 2b and Figure S4). These results confirmed that the protonation is dominant on the 5-membered ring, yielding a stable tropylium cation, in accordance with related findings in literature.[5-7,10] The protonation made the absorption and emission spectra change slightly (Figure S5 and S6). In contrast, these optical properties altered greatly when the sample was photoirradiated.

The *Z*-to-*E* photoisomerization occurs when the tropylium species *Z*-**A_1**H was irradiated by visible light or UV light at 365 nm. With the employment of the ^{1}H-^{1}H COSY spectra to assist the characterizations, the proton resonances can be well assigned in both of the *Z*- and *E*-forms (Figure 2e and 2f). The resultant *E*-isomer was confirmed by the ^{1}H NMR spectrum where a group of upfield shifted resonances of the cyanostyryl-modified azulene skeleton were observed except for proton 1 and 7 (Figure 2c and Figure S7). The peaks of proton 1 and 7 shifted oppositely to the others due to their facing of the electron-withdrawing group -CN in the *E*-form. The maximum photoisomerization efficiency is over 40% according to the NMR integral studies. Upon the irradiation at 365 nm, the *Z*-to-*E* photoisomerization was accelerated and the compound reached a photostationary state shortly within 2 h under at a relatively low power (8 W).

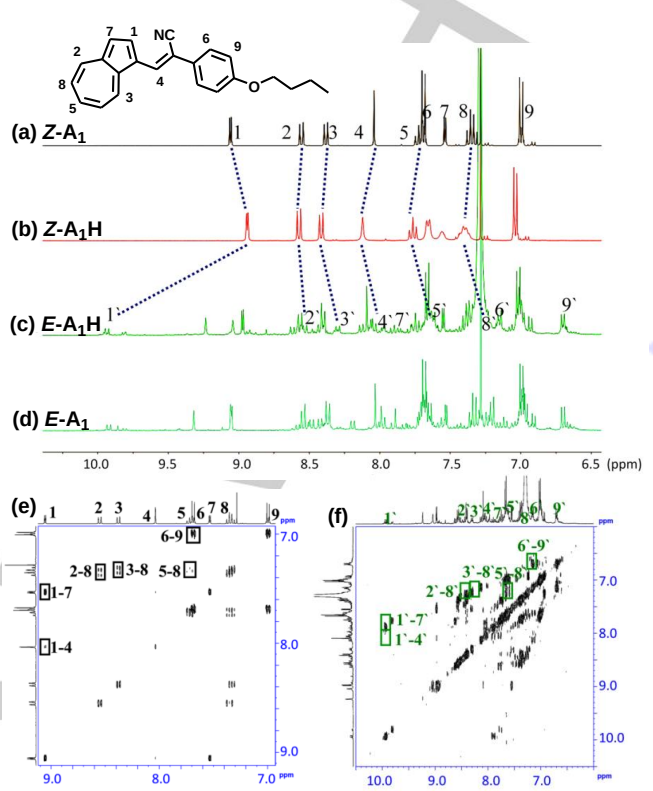

Figure 2. Characterization of the protonation-assistant photoisomerization: ^{1}H NMR spectra (400 MHz, $CDCl_3$) of compound **A_1** (a) at initial state (*Z*-**A_1**), (b) after protonation by TFA (0.3 mol/L, *Z*-**A_1**H), then (c) after photoirradiation (*E*-**A_1**H), and followed by (d) heating (*E*-**A_1**). ^{1}H-^{1}H COSY spectra of (e) *Z*-**A_1** and (f) *E*-**A_1**.

Similar to other photoisomerizable species, [11] the *Z*-to-*E* photoisomerization of compound **A_1** diminishes the main absorption band (~420 nm) of the molecule (see Figure 3a and S8). However, a remarkable absorption band around 680 nm appeared simultaneously in our case (Figure 3a), featuring that the S_0-to-S_1 transition was strengthened by irradiation whereas the S_0-to-S_2 one was suppressed. The remarkable alternation of the different ground-to-excited state transitions can be well distinguished by naked eye (see the solution color change from greenish yellow to dark-green in Figure 3a). Our photoluminescent spectral studies thus revealed that the compound is able to exhibit an enhancement feature. As seen from Figure 3b, the *E*-isomer produces a strong emission at ~480 nm as compared to the relatively quenched emission in its *Z*-isomer (see also the photographs under a UV light in Figure 3b). Here the optical properties along with the protonation-assistant *Z*/*E*-photoisomerization process are clearly featured as the control study without irradiation on the tropylium species that did not show any apparent absorption and emission changes (Figure S10 and S11). The S_0-to-S_1 transition and the significantly intensified emission are maintained after the

deprotonation. These results indicate that the *E*-isomer is also a stable state. It could be converted back to its *Z*-form by heating the sample at high temperature over 65 °C (see Figure S12). The extinction coefficient of the main peaks for compounds *Z*-**A_1**, *E*-**A_1**, *Z*-**A_2**, and *E*-**A_2** are 5.12×10^4, 1.52×10^4, 1.87×10^4 and 7.54×10^3 $M^{-1}cm^{-1}$, respectively.

The change in luminescent intensity is related to conformational restrictions of the *Z/E*-photoisomerization process. Computational studies at the B3LYP/6-31G (d,p) level indicate that a twisted intramolecular charge transfer (TICT) [12] within the cyanostyryl moiety was generated upon photo-excitation of the initial *Z*-isomer, followed by intramolecular rotation of the azulenyl group under no steric hindrance from the opposite phenoxy group with a dihedral angle of 177.6° (Figure 1b). This conformation allows for an efficient nonradiative decay path that leads to quenching of the luminescence. Upon photoisomerization to the *E*-isomer, the TICT pathway was inhibited since the molecular rotation was sterically restricted as evidenced from a relatively rigid conformation with a dihedral angle of 9.6° (Figure 1b),[13] which in turn presents a strong emission. Such photophysics essentially originate from the newly built π-functional skeleton, and compound **A_2** displays the identical optical properties as **A_1** during the *Z/E*-photoisomerization process (Figure S13 and S14). In addition to the major emission band at around 480 nm, the compounds also showed a tunable long-wavelength emission located at the NIR spectral region (~810 nm, see insert of Figure 3b). This signal will be more efficient while also excited by a NIR light power source.

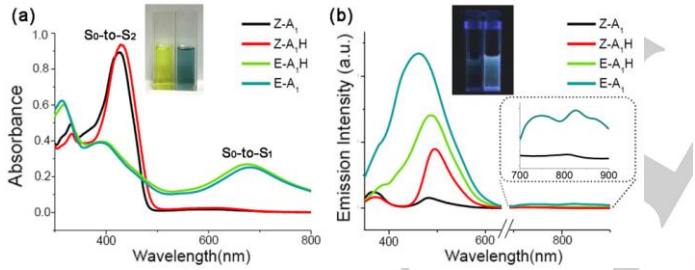

Figure 3. Optical properties along with the protonation-assistant photoisomerization: (a) UV-Vis spectra and (b) emission spectra (λ_{ex}=330 nm) of **A_1** at different states in $CHCl_3$ (5×10^{-5} mol/L) at rt. The insets shows the photographs of the solutions with *Z*- and *E*-forms, respectively, under daylight and a UV light (λ_{ex} = 365 nm). The emission signals in the NIR spectral region of (b) are also highlighted.

Having characterized the tunable optical transition processes along with *Z/E*-isomerization, we now turn to explore the different luminescent behaviors of these molecules. For a potential bioimaging application in vivo, luminescence in water as well as biocompatibility are required. Both the *Z*- and *E*-forms of compound **A_2** can form vesicular nanostructures in water, whereby the hydrophobic π-functional skeleton self-organized internally whereas hydrophilic PEG_{2000} chain exposed to the aqueous environment, as shown by the TEM images (Figure 4a and 4b). Such morphologies are favorable for cell endocytosis without affecting the luminescent signal expressions (vide infra).

In addition to figuring out the tunable visible emission (Figure 3b, 4c and S15), we also explored the NIR emissive pathway by excitation of low energy with appropriate longpass filters applied. Since a chemical channel for rapid relaxation exists in the S_1 state, only emission from higher excited states can be seen for azulene and its derivatives [6] For the present cases, however, a substantial NIR emission around 800 nm was observed in the *E*-form (Figure 4d and S16), the quantum yield of which (~2%) can be evenly matched with that of the visible emission band (3.7%). Such a strong NIR emission can be attributed to 1) the enhancement of the S_0-to-S_1 transition that increases the probability of the radiative decay from the S_1 state (referenced from the UV-Vis spectral change), 2) the conformational restriction of the *E*-form that can be helpful for inhibiting the nonradiative relaxation processes. The time-resolved emission study indicates a fluorescence mechanism with a short lifetime of 5 ns (Figure S17), ensuring the emission can be insensitive to oxidizers or sensitizers (Figure S15 and S16) so as to be fit for better applications in vivo. In contrast, the NIR luminescence cannot be observed when the S_0-to-S_1 transition is unmatched like for the precursors (Figure S18). Thus, dual-pathway (Vis and NIR) luminescence for the unimolecular systems can be realized by structural design and *Z/E*-isomerization (see the proposed illustration in Figure 4f). A kit of dual-pathway luminescent functions is valuable as an optical micro-apparatus for applications, exemplified by the unimolecular selective imaging studies discussed below.

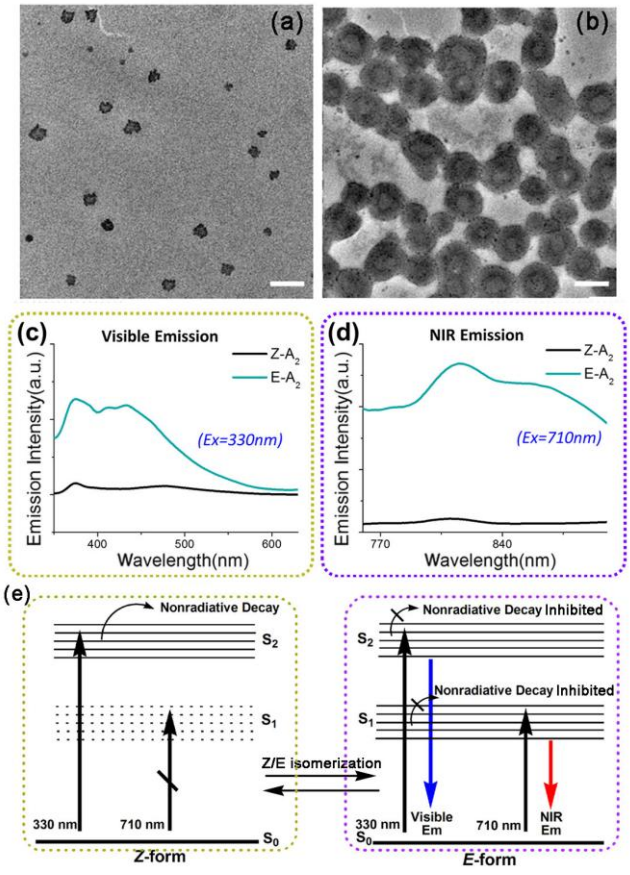

Figure 4. Tuning for dual-pathway luminescence: TEM images of (a) *Z*-**A_2** and (b) *E*-**A_2** prepared from water solution (scale bar: 100 nm). Emission spectra (c: λ_{ex}=330 nm, scanning range = 350 - 900 nm, d: λ_{ex}=710 nm, scanning range = 730 - 900 nm) of **A_2** at *Z*- and *E*-form in water (5×10^{-5} mol/L) at rt. (e) Proposed mechanism for the tuning of the dual-pathway luminescence in *Z*- and *E*-form.

Although tunable imaging techniques have been emerging at the microscale,[14] reports on unimolecular selective imaging under the control of detection channels are still scarce. In our work, experiments in living cells were also carried out to further demonstrate the potential application of the tunable dual-pathway luminescence provided from the unimolecular platform. As compared with those tranditional fluorescent probes (coumarin, diamidinophenylindole, fluorescein, etc.) for biological studies,[15] our system compromises the merits of dual-pathway luminescence and long wavelength (>700 nm) excitation. As in situ photoisomerization of **A_2** undergoes a relatively slow process in acidic internal environments, the incubations of normal MC3T3-E1 cells with compound **A_2** in *Z*- or *E*-form (1×10^{-3} mol/L), in a MEM-α medium at 37 °C for 4 h, were monitored by confocal microscopy (Figure 5) to showcase the selective imaging effect. The results indicate that both of the *Z*- and *E*-forms of **A_2** can be endocytosed by cells for bioimaging (see the images of bright field and each luminescent channels for comparison) with low-cytotoxicity (Figure S19). The cell spreading morphology is quite normal after incubation (see the bright field in Figure 5), further indicating that such a concentration and exposition time did not cause cell damage and apoptosis.

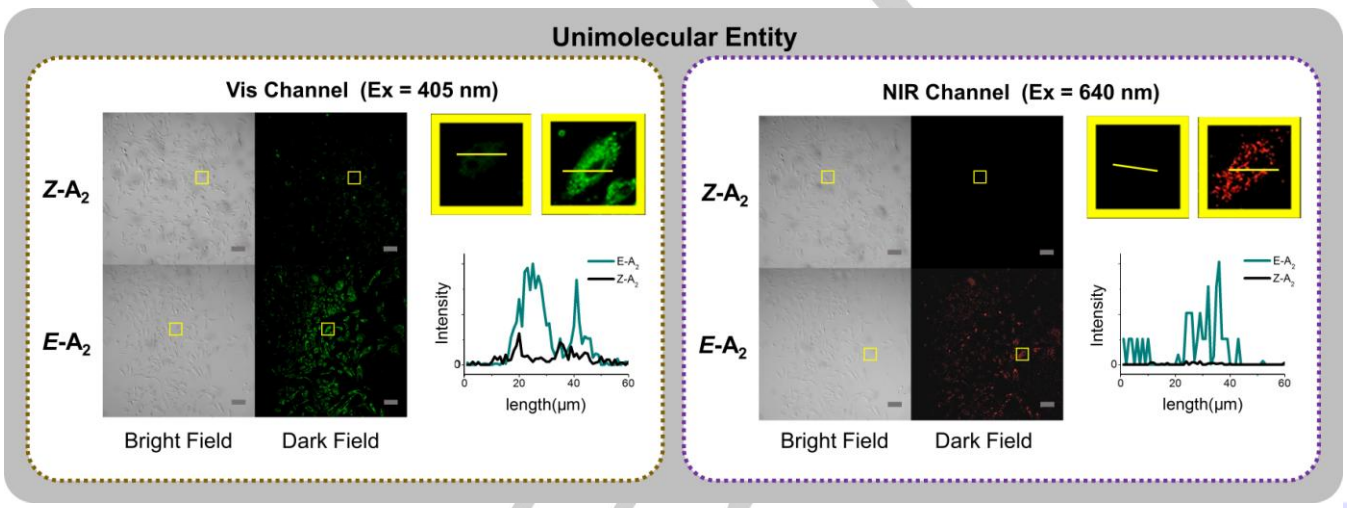

Figure 5. Selective dual-channel imaging: representative results of the unimolecular imagings for MC3T3-E1 cells incubated with compound **A_2** (1×10^{-3} mol/L) from (left) Vis channel and (right) NIR channel, in a MEM-α medium at 37 °C for 4 h. The brightness intensity changes along the lines within the highlighted areas are also displayed. Scale bar, 100 μm.

The effect of selective dual-channel imaging can be detected by confocal microscopes. For the Vis channel, the cell imaging with compound **A_2** in the *E*-form can be clearly observed from the 405 nm excitation, while the imaging of the same channel is relatively weak with **A_2** in the *Z*-form (Figure 5). The tiny brightness from the imaging with **A_2** in *Z*-form may be distributed to the cellular self-luminescent signals. The selective imaging effect from the NIR channel is much remarkable. The imaging with **A_2** in the *Z*-form is completely dark under the 640 nm excitation, whereas it is greatly strengthened with **A_2** in the *E*-form (Figure 5). The luminescent intensity differences along the cellular profile can also be highlighted (Figure 5). As we demonstrated above, the *Z*/*E* isomerization allows the emission of the materials to undergo a significant intensity change both in the Vis and NIR spectral regions. This exploration suggests that the conformationally depended photophysical alternation process also can occur at the cell level, in agreement with the corresponding photoluminescent behavior in solution. Such spectrally tunable unimolecular entities might thus present a promising potential for biomaterial applications at the microscale.

In summary, a cyanostyryl-modified azulene system with in situ stimuli response and tunable photophysical behavior has been designed and developed. NIR emissive fashion was opened in this system and consequently a dual-pathway (Vis and NIR) luminescent strategy with intensity adjustable was developed, whereby two factors: the S_0-to-S_1 transition regulation and control of molecular conformation, play key roles. The tunable Vis-NIR emission takes place on a unimolecular entity. Selective dual-channel imaging using the smart compound has been demonstrated through intracellular studies. The present interdisciplinary results can be valuable for inspiring new design or development of organic intelligent materials with potential applications for multi-mode light-emission.

Acknowledgements

This work was supported by the NSFC/China (21644005), National Program for Thousand Young Talents of China, and State Key Project of Research and Development

(2016YFC1100300). Y. Z. acknowledges NSFC/China (21502229) and China Postdoctoral Science Foundation funded project (2016M601491) for additional research supports. X. L. and H.Å. thank the Swedish National Infrastructure for Computing (SNIC) for providing computational resources for project SNIC 2014-11/31. Y. Z. and L.Z thanks Prof. M. Ji and Prof. H. Zhu for helpful discussions.

Keywords: dual-pathway emission • azulene • nearinfrared luminescence • *Z/E*-isomerization • selective imaging

[1] a) X. Michalet, F. F. Pinaud, L. A. Bentolila, J. M. Tsay, S. Doose, J. J. Li, G. Sundaresan, A. M. Wu, S. S. Gambhir, S. Weiss, *Science* **2005**, *307*, 538-544; b) T. Pozzan, *Nature* **1997**, *388*, 834-835; c) Y. You, S. Lee, T. Kim, K. Ohkubo, W. S. Chae, S. Fukuzumi, G. J. Jhon, W. Nam, S. J. Lippard, *J. Am. Chem. Soc.* **2011**, *133*, 18328-18342; d) M. Q. Zhu, G. F. Zhang, C. Li, M. P. Aldred, E. Chang, R. A. Drezek, A. D. Li, *J. Am. Chem. Soc.* **2011**, *133*, 365-372; e) Z. Chang, L. Jing, B. Chen, M. Zhang, X. Cai, J. Liu, Y. Ye, X. Lou, Z. Zhao, B. Liu, J. Wang, B. Z. Tang, *Chem. Sci.* **2016**, *7*, 4527-4536; f) Q. T. Nguyen, E. S. Olson, T. A. Aguilera, T. Jiang, M. Scadeng, L. G. Ellies, R. Y. Tsien, *Proc. Natl. Acad. Sci. USA* **2010**, *107*, 4317-4322; g) G. Song, C. Liang, H. Gong, M. Li, X. Zheng, L. Cheng, K. Yang, X. Jiang, Z. Liu, *Adv. Mater.* **2015**, *27*, 6110-6117; h) H. Wu, P. Zhao, X. Li, W. Chen, H. Agren, Q. Zhang, L. Zhu, *ACS Appl. Mater. Inter.* **2017**, *9*, 3865-3872; i) Y. Yang, Q. Zhao, W. Feng, F. Li, *Chem. Rev.* **2013**, *113*, 192-270.

[2] a) S. A. Hilderbrand, R. Weissleder, *Curr. Opin. Chem. Biol.* **2010**, *14*, 71-79; b) X. Wu, X. Sun, Z. Guo, J. Tang, Y. Shen, T. D. James, H. Tian, W. Zhu, *J. Am. Chem. Soc.* **2014**, *136*, 3579-3588; c) L. Yuan, W. Lin, K. Zheng, L. He, W. Huang, *Chem. Soc. Rev.* **2013**, *42*, 622-661; d) X. Chen, X. Tian, I. Shin, J. Yoon, *Chem. Soc. Rev.* **2011**, *40*, 4783-4804; e) K. Kiyose , H. Kojima , T. Nagano *Chem. -Asian J.* **2008**, *3*, 506-515.

[3] a) S. Sreejith, K. P. Divya, A. Ajayaghosh, *Angew. Chem.* **2008**, *120*, 8001-8005; b) W. M. Leevy, S. T. Gammon, H. Jiang, J. R. Johnson, D. J. Maxwell, E. N. Jackson, M. Marquez, D. Piwnicaworms, B. D. Smith, *J. Am. Chem. Soc.* **2006**, *128*, 16476-16477; c) C. K. Lim, S. Kim, I. C. Kwon, C. H. Ahn, S. Y. Park, *Chem. Mater.* **2009**, *21*, 5819-5825; d) J. O. Escobedo, O. Rusin, S. Lim, R. M. Strongin, *Curr. Opin. Chem. Biol.* **2010**, *14*, 64-70.

[4] a) Z. Zhang, B. Xu, J. Su, L. Shen, Y. Xie, H. Tian, *Angew. Chem. Int. Ed. Engl.* **2011**, *50*, 11654-11657; b) B. Shi, K. Jie, Y. Zhou, J. Zhou, D. Xia, F. Huang, *J. Am. Chem. Soc.* **2016**, *138*, 80-83.

[5] a) E. Puodziukynaite, H. W. Wang, J. Lawrence, A. J. Wise, T. P. Russell, M. D. Barnes, T. Emrick, *J. Am. Chem. Soc.* **2014**, *136*, 11043-11049; b) E. Amir, R. J. Amir, L. M. Campos, C. J. Hawker, *J. Am. Chem. Soc.* **2011**, *133*, 10046-10049; c) Y. Yamaguchi, K. Ogawa, K. Nakayama, Y. Ohba, H. Katagiri, *J. Am. Chem. Soc.* **2013**, *135*, 19095-19098.

[6] a) T. Itoh, *Chem. Rev.* **2012**, *112*, 4541-4568; b) X. Zhang, C. Li, W. Wang, X. Cheng, X. Wang, B. Zhang, *J. Mater. Chem.* **2007**, *17*, 642-649; c) T. Tang, T. Lin, F. Wang, C. He, *J. Phys. Chem. B* **2015**, *119*, 8176-8183.

[7] a) J. Xia, B. Capozzi, S. Wei, M. Strange, A. Batra, J. R. Moreno, R. J. Amir, E. Amir, G. C. Solomon, L. Venkataraman, L. M. Campos, *Nano Lett.* **2014**, *14*, 2941-2945; b) K. Tsurui, M. Murai, S. Ku, C. J. Hawker, M. J. Robb, *Adv. Funct. Mater.* **2014**, *24*, 7338-7347; c) F. Wang, T. Lin, C. He, H. Chi, T. Tang, Y.-H. Lai, *J. Mater. Chem.* **2012**, *22*, 10448-10451; d) E. Amir, M. Murai, R. J. Amir, J. S. Cowart, M. L. Chabinyc, C. J. Hawker, *Chem. Sci.* **2014**, *5*, 4483-4489.

[8] a) B. K. An, J. Gierschner, S. Y. Park, *Acc. Chem. Res.* **2012**, *45*, 544-554; b) L. Zhu, X. Li, Q. Zhang, X. Ma, M. Li, H. Zhang, Z. Luo, H. Agren, Y. Zhao, *J. Am. Chem. Soc.* **2013**, *135*, 5175-5182; c) L. Zhu, Y. Zhao, *J. Mater. Chem.* **2013**, *1*, 1059-1065; d) A. K. Mandal, S. Sreejith T. He, S. K. Maji, X. J. Wang, S. L. Ong, J. Joseph, H. Sun, Y. Zhao, *ACS NANO* **2015**, *9*, 4796-4805; e) C. Hang, H. Wu, L. Zhu, *Chinese Chem. Lett.* **2016**, *27*, 1155-1165.

[9] J. Saltiel, D. H. Ko, S. A. Fleming, *J. Am. Chem. Soc.* **1994**, *116*, 4009-4010.

[10] M. Murai, E. Amir, R. J. Amir, C. J. Hawker, *Chem. Sci.* **2012**, *3*, 2721-2721.

[11] a) L. Zhu, H. Yan, K. T. Nguyen, H. Tian, Y. Zhao, *Chem. Commun.* **2012**, *48*, 4290-4292; b) H. Yan, C. Teh, S. Sreejith, L. Zhu, A. Kwok, W. Fang, X. Ma, K. T. Nguyen, V. Korzh, Y. Zhao, *Angew. Chem. Int. Ed. Engl.* **2012**, *51*, 8373-8377; c) L. Zhu, X. Ma, F. Ji, Q. Wang, H. Tian, *Chem. -Eur. J.* **2007**, *13*, 9216-9222; d) L. Zhu, X. Li, S. Wu, K. T. Nguyen, H. Yan, H. Agren, Y. Zhao, *J. Am. Chem. Soc.* **2013**, *135*, 9174-9180.

[12] a) Z. R. Grabowski, K. Rotkiewicz, W. Rettig, *Chem. Rev.* **2003**, *103*, 3899-4032; b) W. Zhang, Z. Lan, Z. Sun, K. J. Gaffney, *J. Phys. Chem. B* **2012**, *116*, 11527-11536.

[13] a) L. L. Zhu, X. Li, F. Y. Ji, X. Ma, Q. C. Wang, H. Tian, *Langmuir* **2009**, *25*, 3482-3486; b) L. Zhu, C. Y. Ang, X. Li, K. T. Nguyen, S. Y. Tan, H. Agren, Y. Zhao, *Adv. Mater.* **2012**, *24*, 4020-4024; c) L. Zhu, D. Qu, D. Zhang, Z. Chen, Q. Wang, H. Tian, *Tetrahedron* **2010**, *66*, 1254-1260.

[14] a) B. Wang, J. Hai, Z. Liu, Q. Wang, Z. Yang, S. Sun, *Angew. Chem. Int. Ed. Engl.* **2010**, *49*, 4576-4579; b) W. Shi, X. Li, H. Ma, *Angew. Chem. Int. Ed. Engl.* **2012**, *51*, 6432-6435.

[15] a) X. Zhang, Q. Ba, Z. Gu, D. Guo, Y. Zhou, Y. Xu, H. Wang, D. Ye, H. Liu, *Chem. -Eur. J.* **2015,** *21*, 17415-17421; b) A. Tirla, P. Rivera-Fuentes, *Angew. Chem. Int. Ed.* **2016,** *55*, 14709-14712; c) W. Shen, J. Luan, L. Cao, J. Sun, L. Yu, J. Ding, *Biomacromolecules* **2015**, *16*, 105−115.

10.1002/chem.201700947

WILEY-VCH

COMMUNICATION

*Yunyun Zhou, Yaping Zhuang, Xin Li, Hans Ågren, Lin Yu, Jiandong Ding, Liangliang Zhu**

Selective Dual-Channel Imaging on Cyanostyryl -Modified Azulene Systems with Unimolecularly Tunable Visible-Nearinfrared Luminescence

By integrating an azulene and a cyanostyryl moiety into one skeleton, we employed the excited-state regulation and conformational control via stimuli-responsive push-pull effect to enable the generation of NIR emissive channel of the azulene system, so as to address the dual-pathway (Vis and NIR) emission on unimolecular scaffold and a well application in selective dual-channel cell imaging.